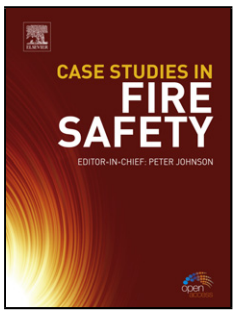

Title: In-coating graphene nano-platelets for environmentally-friendly corrosion protection of iron

Author: C.F. Glover C. Richards J. Baker G. Williams H.N. McMurray

PII: S0010-938X(16)31177-5
DOI: http://dx.doi.org/doi:10.1016/j.corsci.2016.11.009
Reference: CS 6936

To appear in:

Received date: 1-6-2016
Revised date: 24-10-2016
Accepted date: 14-11-2016

Please cite this article as: C.F.Glover, C.Richards, J.Baker, G.Williams, H.N.McMurray, In-coating graphene nano-platelets for environmentally-friendly corrosion protection of iron, Corrosion Science http://dx.doi.org/10.1016/j.corsci.2016.11.009

In-coating graphene nano-platelets for environmentally-friendly corrosion protection of iron

C.F. Glover*, C.Richards, J.Baker

SPECIFIC, Baglan innovation Centre, Central Avenue, Baglan Energy Park, Baglan, Port Talbot, SA12 7AX.

G. Williams, H.N. McMurray

Materials Research Centre, College of Engineering, Swansea University, Bay Campus, Fabian Way, Swansea, UK, SA1 8EN.

*Corresponding author: Tel: 07941608125
E-mail address: C.F.Glover@swansea.ac.uk

Highlights

- GNP-pigmented films show exceptional resistance to cathodic delamination.
- Oxygen-diffusion shown to be the rate-limiting step in the presence of GNPs.
- Delamination rates correlate with through-coating oxygen permeation rates.

A primer coating system adherent to iron substrates based on graphene nano-platelets (GNPs) dispersed in polyvinylbutyral (PVB) is presented. Using a scanning Kelvin probe (SKP), the composite coatings are shown to exhibit exceptional resistance to an important corrosion-driven failure process, namely cathodic delamination, when aqueous chloride electrolyte is introduced to a penetrating coating defect. Delamination rate kinetics are shown to correlate strongly with reductions in the rate of oxygen permeation through the coating with increasing GNP pigment volume fraction.

Keywords: Graphene nano-platelets, corrosions, scanning Kelvin probe, cathodic delamination, iron.

1. Introduction

Recent interest in graphene as an additive to organic coatings for application to metal surfaces for protection against corrosion has led to a number of intriguing and high-level publications [1-3]. Here we demonstrate, using Scanning Kelvin probe (SKP) measurements, that composite coatings based on non-functionalised graphene nano-platelet (GNP) pigmented polyvinyl butyral (PVB) films show exceptional resistance to an important corrosion-driven failure process - namely cathodic delamination. We further demonstrate that delamination rates correlate strongly with reductions in the rate of oxygen permeation through the coating. The current paper describes a novel primer coating system for iron

substrates based on GNPs prepared in a manner where a low pressure, low temperature, split plasma exfoliation treatment has been adopted [4].

Figure 1

Failure of organic coating adhesion by cathodic delamination, shown schematically in **Figure 1**, is driven forward via cathodic oxygen reduction (COR) occurring at the metal-coating interface [5-7]. Conventional corrosion-inhibitor pigments (such as Cr(VI)) typically act by chemically inhibiting cathodic electron transfer to oxygen. However, various studies have claimed that the benefits of graphene and graphene-composites for corrosion protection arise principally from reduced permeation to oxygen and water [1, 8–11]. In the current study, an experimental arrangement, namely the scanning Kelvin probe (SKP) technique, is used which allows free ingress of corrosive electrolyte via an artificial coating defect so that the influence of oxygen permeation on the COR rate can be determined in isolation. SKP is now a firmly-established methodology following the kinetics of corrosion-driven organic coating failure/delamination [12-16] and, indeed, for other corrosion studies [17-19]. In the current study, we use SKP to assess the effect of systematically varying the GNP content of GNP/PVB composite coatings adherent to an iron substrate in contact with high humidity (95%) air. PVB has been used extensively as a model coating in previous studies into the inhibition of corrosion-driven underfilm delamination [20].

Oxygen permeation rates are also independently measured for free-standing GNP/PVB films using a photochemical technique. For the first time, a direct correlation between the rate of corrosion-driven coating delamination and oxygen permeability is demonstrated. It is therefore proposed that GNPs act principally to reduce the COR rate by limiting the rate at which oxygen can diffuse to the metal coating interface (**Figure 1.a**).

2. Materials and methods

Materials: Iron samples, obtained from Goodfellow, were a gauge of 1.5 mm cut into square coupons of 50 mm × 50 mm. All chemicals were supplied by Sigma-Aldrich Chemical Co and were of analytical grade purity. GNPs, with average surface area of 17 m^2g^{-1} obtained from Haydale ltd were dispersed in PVB at various pigment volume fractions (ϕ_{PT}) calculated using:

$$\phi_{PT} = \left(1 + \frac{M_{PVB}.\rho_{PT}}{M_{PT}.\rho_{PVB}}\right)^{-1} \qquad \text{eq. [1]}$$

where M_{PVB} is the mass of PVB used in the coating formulation, M_{PT} the mass of GNP pigment ρ_{PVB} the density of PVB (~ 0.8 g cm^{-3})[21] and ρ_{PT} the density of the GNP pigments (~ 2.25 g cm^{-3}).

Methods: SKP design and operation of apparatus has been described extensively elsewhere [13][22-23], as has the SKP calibration procedure in terms of free corrosion potential (E_{corr}) [20]. It has been shown, for a metal surface coated with an adherent and/or delaminated PVB film, that:

$$E_{corr} = \Delta\psi_{Pol}^{Ref} + A \text{ V(SHE)} \qquad \text{eq. [2]}$$

where $\Delta\psi_{Pol}^{Ref}$ is the Volta potential difference measured between the SKP reference probe and the polymer-air interface and A is a constant.

The sample preparation procedure was based on the methods presented in work carried out by Klimow et al [14]. Polyvinyl butyral (PVB) solutions MW 70,000-100,000 were prepared in ethanol (15.5% w/w) and the required amount of GNPs were added and thoroughly mixed. An aqueous slurry of 5 μm alumina was used to hand-polish the sample surface to remove

any contaminants and a pre-existing oxide layer. Degreasing was carried out via an acetone rinse followed by air-drying. PVB solution containing the appropriate amount of GNPs was bar-cast onto a pre-cleaned sample and room-air dried. Strong film adhesion was observed in both wet and dry form where it was not possible for the film to be peeled off.

All delamination experiments were carried out in an enclosed SKP chamber maintained at a constant 95% r.h. and 25˚C. Delamination was initiated each time using 0.86 M wt/v aqueous NaCl at pH 7. The SKP reference probe consisted of a gold wire of diameter 125 µm vibrating vertically at 280 Hz and amplitude of 40 µm at a distance of 100 µm above the sample surface. E_{corr} data points were recorded at 20 per mm. The SKP reference probe was scanned over the coated surface along a 12 mm line normal to, and adjacent with, the defect-coating boundary. Scanning commenced immediately on the addition of electrolyte and thereafter at hourly intervals over a period of $\geq$ 24h.

A photochemical technique based on the "methylene blue bottle reaction" was employed to determine the oxygen permeability of the GNP/PVB films [24]. This technique relies on the fact that Methylene blue (MB), when exposed to red light in the presence of a sacrificial reducing agent, becomes reduced to its leuco, colourless form. Upon exposure to oxygen it is stoichiometrically reoxidised to MB. A Hellma 10 mm 100 QS quartz cuvette was filled with $2x10^{-5}$ M aqueous MB and $1x10^{-3}$ M aqueous EDTA adjusted to pH 10 using aqueous NaOH. A free-standing PVB film containing the relevant volume fraction of GNPs (φ_{GNP}) was then sealed over the cuvette mouth using epoxy adhesive. All sample preparation was carried out in a nitrogen atmosphere and residually resolved oxygen removed by repeatedly photo-bleaching the MB until it became completely colourless. The cuvette was then allowed to stand in air at room temperature pressure and MB recolourisation following spectrophotometry. The MB peak absorbance occurs at a wavelength of 662 nm with an

extinction coefficient of 73,000 [25]. A Lambda XLS Perkin Elmer UV/Vis spectrophotometer was used to measure the MB absorbance change at 15 minute intervals for two hours. A baseline for oxygen leakage through the epoxy adhesive was obtained using a glass cover-slip instead of the PVB/GNP film.

3. Results and discussion

By placing an experimental electrolyte comprising 0.86 M aqueous sodium chloride onto a penetrative coating defect, an electrochemical cell becomes established, as shown in Figure 1. Coating delamination then occurs by the galvanic coupling of anodic metal dissolution in the defect region with cathodic oxygen reduction occurring at the advancing delamination front (Eq. 3 and Eq. 4 respectively). The electrochemical reduction of molecular O_2 leads to the generation of OH^- ions that render the cathodic delamination zone highly alkaline (i.e. > pH 10)[5,6] . Disbondment occurs initially via the formation of hydroxyl radicals that form as a result of the cathodic reduction of oxygen causing oxidative degradation of the organic binder. A thin, gel-like layer of electrolyte ingresses underneath the coating and loss of adhesion is widely attributed to alkaline attack on the coating-metal bond [6][26] (Eq. 4).

$$Fe \rightleftharpoons Fe^{2+} + 2e^- \qquad \text{eq. [3]}$$

$$O_2 + 2\,H_2O + 4e^- \rightleftharpoons 4OH^- \qquad \text{eq. [4]}$$

Initially, measurements on unpigmented PVB coatings were performed to obtain baseline delamination kinetics (**Figure 2.a**). Upon establishment of an equilibrium between the coating and the humid atmosphere, corrosion potential (E_{corr}) values measured over the intact coating surface, observed in the 'intact' region of Figure 2.a**,** are uniformly high (i.e. ca. 0.1 – 0.2 V(SHE)). Following electrolyte introduction at the coating defect, delamination typically became initiated within 2 h and distinctive time-dependent E_{corr} vs. distance profiles

developed.

The E_{corr} values measured in the vicinity of the defect, determined by the dynamic equilibrium of iron oxidation and oxygen reduction, results in a potential that approaches the equilibrium potential of eq. [3] i.e. ca. -0.44 V(SHE). The position of the delamination front is taken as the midpoint of the sharp drop in potential from the intact coating region, as described previously by Leng et al [26].

Figure 2

Figure 2.b, shows representative E_{corr} vs. delamination distance (x_{del}) profiles for a coating containing a GNP volume fraction (φ_{GNP}) of 0.054. A delamination distance (x_{del}) of only 1 mm was produced after a holding period of 24 h. Delamination kinetics were determined by plotting delaminated distance (x_{del}) against the time minus the time for delamination to become initiated (t_{del} - t_i) (**Figure 3.a**). For uninhibited PVB coatings, it has previously been demonstrated that delamination from an iron surface is controlled by the underfilm migration of cations (in this case Na^+) from the defect site to the cathodic delamination front[26], giving rise to parabolic delamination rate kinetics in which x_{del} increases as $t^{1/2}$.

When GNP pigments were introduced into the coating, a marked change was observed in the delamination kinetics. Systematically increasing φ_{GNP} was found to produce a progressive reduction in delamination rate and a change in kinetic order, with respect to time, from parabolic ($t^{1/2}$ dependence) to zero order (linear with respect to t). These effects are clearly shown in Figure 3.a. Only the unpigmented PVB plot shows a deviation from linearity. Linear rate constants (k_{del}), obtained from the various x_{del} vs. (t_{del} - t_i) slopes in Figure 3.a (taken as the initial rate slope in the case of φ_{GNP} = 0 where it is assumed that, as x_{del} and cation diffusion length tends to zero, underfilm cation diffusion ceases to be rate limiting),

are plotted vs. φ_{GNP} in **Figure 3.b** curve (i), which shows that for $\varphi_{GNP} \geq 0.1$ k_{del} values are reduced by $\geq 98\%$ relative to the $\varphi_{GNP} = 0$ case.

Figure 3

Although the delamintation rate is significantly reduced relative to the unpigmented PVB, SKP measurements revealed no dependence of characteristic E_{corr} values on φ_{GNP}. Thus, in Figure 2.b, E_{corr} values in the intact coating region (E_{intact}) remain at 0.1 - 0.2 V(SHE) and E_{corr} in the defect region remains at ~ -0.4 V(SHE). Consequently, there is no reason to propose that GNPs act by exerting any electronic effect or by directly influencing any interfacial electron transfer processes.

Given the above, the simplest explanation of the inhibitory action of GNPs is that they act to reduce rates of vertical (through coating) oxygen diffusion as shown schematically in Figure 1.a. This hypothesis is immediately consistent with the diffusion blocking effects of GNPs in polymer composite films reported by Kirkland [1]. Further support is provided by curve (ii) in Figure 3.b which shows oxygen permeability coefficiencies measured for free-standing films vs. φ_{GNP}. A comparison of curves (i and ii) then illustrates the main degree of correlation which exists between k_{del} and oxygen permeability.

It has been pointed out that, when protective coatings function principally on reduced rates of oxygen diffusion, long-term corrosion resistance is unlikely to occur [27]. Consequently, the graphene pigmented PVB coatings are currently being subjected to scribed-sample salt-spray testing to evaluate their long-term performance.

3. Conclusion

In conclusion, *in-situ* scanning Kelvin probe (SKP) experiments have demonstrated that

Graphene Nanooplatelets (GNPs), dispersed in a polyvinyl butyral (PVB) primer coating, can effectively inhibit the corrosion-driven organic coating cathodic delamination mechanism on an iron surface. In the presence of 0.124 φ_{GNP}, the highest GNP volume fraction used in this study, the delamination rate was reduced by 98.6%. Analysis of delamination rate kinetics reveals a change from parabolic to linear suggesting that, in the presence of GNPs, the diffusion of Oxygen to the cathodic site is the rate limiting step. Oxygen permeation data supports this theory, demonstrating a direct correlation between corrosion-driven delamination rate and the diffusion of oxygen through the coating.

5. Acknowledgements

The authors recognise the financial support of the EPSRC, Welsh Government and Innovate UK for the SPECIFIC Innovation and Knowledge Centre (grant numbers EP/I019278/1, EP/K000292/1, EP/L010372/1). The authors would also like to thank Haydale Ltd for providing the materials.

5. References

[1] N.T. Kirkland, T. Schiller, N. Medhekar, N. Birbilis, Exploring graphene as a corrosion protection barrier, Corros. Sci. 56 (2012) 1–4.

[2] S. Böhm, Graphene against corrosion., Nat. Nanotechnol. 9 (2014) 741–2.

[3] B.R. V Dennis, L.T. Viyannalage, V. Anil, Nanocomposite Coatings for Protecting Low- Alloy Steels From Corrosion, Am. Ceram. Soc. Bull. 92 (2013) 18–24.

[4] M. Williams, K. Seunarine, R. Gibbs, C. Spacie, Plasma modification of graphene and graphene like materials for component performance enhancement, Nano Res. 27 (2013) 23–27.

[5] G. Williams, N. McMurray, Underfilm/coating coating, Shreir's Corros. 2 (2009) 988–1004.

[6] G. Grundmeier, W. Schmidt, M. Stratmann, Corrosion protection by organic coatings : electrochemical mechanism and novel methods of investigation, Electrochim. Acta. 45 (2000) 2515–2533.

[7] J. Marsh, J.D. Scantlebury, S.B. Lyon, The effect of surface / primer treatments on the performance of alkyd coated steel, 43 (2001) 829–852.

[8] K.C. Chang, M.H. Hsu, H.I. Lu, M.C. Lai, P.J. Liu, C.H. Hsu, W.F. Ji, T.L. Chuang, Y. Wei, J.M. Yeh, W.R. Liu, Room-temperature cured hydrophobic epoxy/graphene composites as corrosion inhibitor for cold-rolled steel, Carbon N. Y. 66 (2014) 144–153.

[9] M. Yi, Z. Shen, X. Zhao, L. Liu, S. Liang, X. Zhang, Exploring few-layer graphene and graphene oxide as fillers to enhance the oxygen-atom corrosion resistance of composites., Phys. Chem. Chem. Phys. 16 (2014) 11162–7.

[10] D. Prasai, J.C. Tuberquia, R.R. Harl, G.K. Jennings, B.R. Rogers, K.I. Bolotin, Graphene: corrosion-inhibiting coating., ACS Nano. 6 (2012) 1102–8.

[11] V. Berry, Impermeability of graphene and its applications, Carbon N. Y. 62 (2013) 1–10.

[12] W. Furbeth, M. Stratmann, The delamination of polymeric coatings from electrogalvanised steel - a mechanistic approach. Part 1: delamination from a defect with intact zinc layer, Corros. Sci. 43 (2001) 207–227.

[13] W. Furbeth, M. Stratmann, The delamination of polymeric coatings from electrogalvanized steel - a mechanistic approach. Part 2: delamination from a defect down to steel, Corros. Sci. 43 (2001) 229–241.

[14] G. Klimow, N. Fink, G. Grundmeier, Electrochemical studies of the inhibition of the cathodic delamination of organically coated galvanised steel by thin conversion films, Electrochim. Acta. 53 (2007) 1290–1299.

[15] H.N. McMurray, D. Williams, G. Williams, D.A. Worsley, Inhibitor pretreatment synergies demonstrated using a scanning Kelvin probe technique, Corros. Eng. Sci. Technol. 38 (2003) 112–118.

[16] G. Williams, H.N. McMurray, M.J. Loveridge, Inhibition of corrosion-driven organic coating disbondment on galvanised steel by smart release group II and Zn(II)-exchanged bentonite pigments, Electrochim. Acta. 55 (2010) 1740–1748.

[17] M. Rohwerder, S. Isik-Uppenkamp, C. A. Amarnath, Application of the Kelvin Probe method for screening the interfacial reactivity of conducting polymer based coatings for corrosion protection, Electrochim. Acta. 56 (2011) 1889–1893.

[18] M. Rohwerder, L.M. Duc, A. Michalik, In situ investigation of corrosion localised at the buried interface between metal and conducting polymer based composite coatings,

Electrochim. Acta. 54 (2009) 6075–6081.

[19] M. Rohwerder, S. Isik-Uppenkamp, M. Stratmann, Application of SKP for in situ monitoring of ion mobility along insulator/insulator interfaces, Electrochim. Acta. 54 (2009) 6058–6062.

[20] G. Williams, H.N. McMurray, Chromate Inhibition of Corrosion-Driven Organic Coating Delamination Studied Using a Scanning Kelvin Probe Technique, J. Electrochem. Soc. 148 (2001) B377.

[21] H. Dominighaus, Plastics for engineers, Munich, (1988) 142.

[22] W. Fürbeth, M. Stratmann, Scanning Kelvin Probe investigations on the delamination of polymeric coatings from metallic surfaces, Prog. Org. Coatings. 39 (2000) 23–29.

[23] M. Stratmann, A. Leng, W. Fürbeth, H. Streckel, H. Gehmecker, K.-H. Groβe-Brinkhaus, The scanning Kelvin probe; a new technique for the in situ analysis of the delamination of organic coatings, Prog. Org. Coatings. 27 (1996) 261–267.

[24] G. Ensell, Photoreduction of Methylene Blue by Ethylenediaminetetraacetic, J. Am. Chem. Soc. 157 (2000) 7–9.

[25] K. Basavaiah, U.R. Anil Kumar, K. Tharpa, K.B. Vinay, Validated spectrophotometric methods for the determination of raloxifene hydrochloride in pharmaceuticals, J. Chil. Chem. Soc. 53 (2008) 1635–1639.

[26] A. Leng, H. Streckel, K. Hofmann, M. Stratmann, The delamination of polymeric coatings from steel Part 3: Effect of the oxygen partial pressure on the delamination reaction and current distribution at the metal/polymer interface, Corros. Sci. 41 (1998) 599–620.

[27] M. Schriver, W. Regan, W.J. Gannett, A.M. Zaniewski, M.F. Crommie, A. Zettl, Graphene as a long-term metal oxidation barrier: Worse than nothing, ACS Nano. 7

(2013) 5763–5768.

List of Figures

Figure 1 Schematic representation of the corrosion-driven delamination cell showing correspondence with various regions of the time-dependent E_{corr} profile. a) Schematic demonstration of increased through-coating tortuosity for oxygen when coatings are loaded with GNPs.

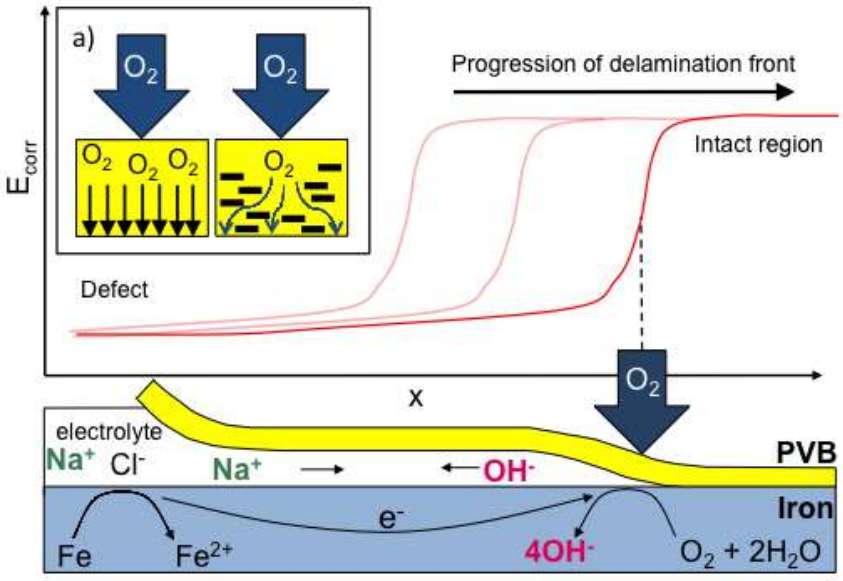

Figure 2. Plots of time-dependent E_{corr} vs. distance from the defect (x) profiles recorded for PVB coatings adherent to iron substrates where a) is the unpigmented coating given at 3 hourly intervals and b) containing 0.054 $\varphi_{GNP,}$ shown at 4 hourly intervals, up to 24 h in both cases.

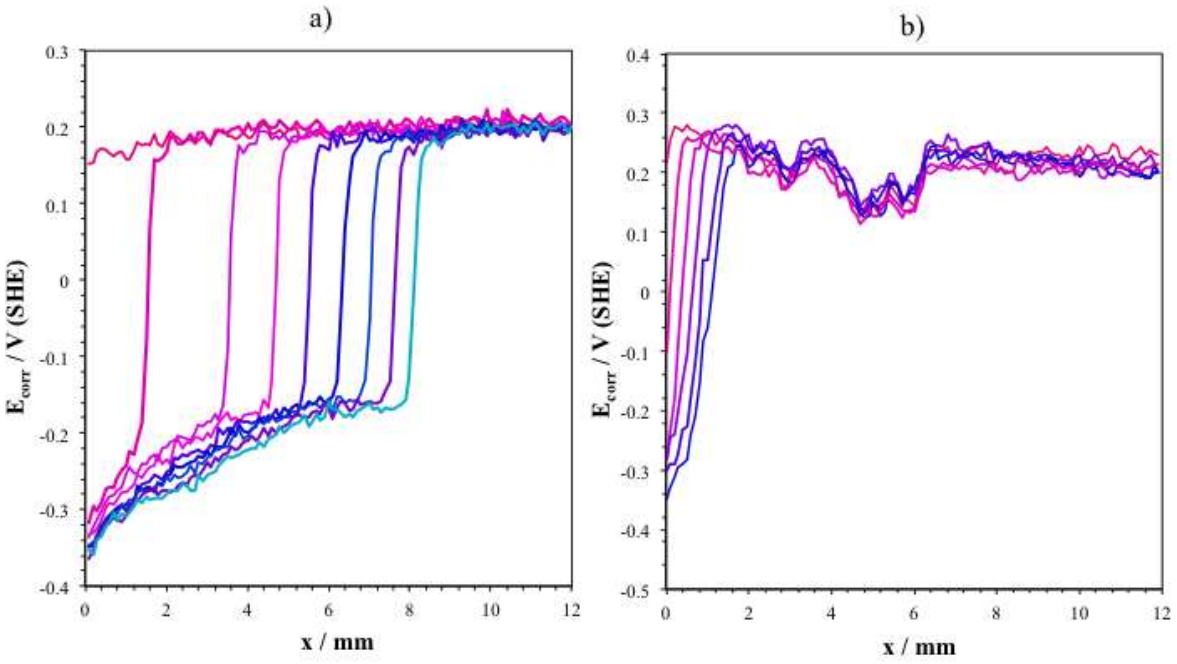

Figure 3.a) Plots of delamination distance (x_{del}) as a function of time (t_{del} - t_i) for PVB coatings containing various φ_{GNP} on iron substrates where 0.86 M aqueous NaCl electrolyte at pH 7.

b) Summary plots of (i) k_{del} and (ii) Oxygen Permeability as a function of φ_{GNP}.